

A novel Si-rich SiN bilayer passivation with thin-barrier AlGaN/GaN HEMTs for high performance millimeter-wave applications

Zhihong Chen(陈治宏), Minhan Mi(宓珉瀚), Jielong Liu(刘捷龙), Pengfei Wang(王鹏飞), Yuwei Zhou(周雨威), Meng Zhang(张濛), Xiaohua Ma(马晓华), and Yue Hao(郝跃)

Citation: Chin. Phys. B, 2022, 31 (**11**): 117105. DOI: 10.1088/1674-1056/ac81a6

What follows is a list of articles you may be interested in

High linearity AlGaN/GaN HEMT with double-V_{th} coupling for millimeter-wave applications

Pengfei Wang(王鹏飞), Minhan Mi(宓珉瀚), Meng Zhang(张濛), Jiejie Zhu(祝杰杰), Yuwei Zhou(周雨威), Jielong Liu(刘捷龙), Sijia Liu(刘思佳), Ling Yang(杨凌), Bin Hou(侯斌), Xiaohua Ma(马晓华), and Yue Hao(郝跃)

Chin. Phys. B, 2022, 31 (**2**): 027103. DOI: 10.1088/1674-1056/ac2b21

High-frequency enhancement-mode millimeterwave AlGaN/GaN HEMT with an f_T/f_{max} over 100 GHz/200 GHz

Sheng Wu(武盛), Minhan Mi(宓珉瀚), Xiaohua Ma(马晓华), Ling Yang(杨凌), Bin Hou(侯斌), and Yue Hao(郝跃)

Chin. Phys. B, 2021, 30 (**8**): 087102. DOI: 10.1088/1674-1056/ac04a5

Modified model of gate leakage currents in AlGaN/GaN HEMTs

Yuan-Gang Wang(王元刚), Zhi-Hong Feng(冯志红), Yuan-Jie Lv(吕元杰), Xin Tan(谭鑫), Shao-Bo Dun(敦少博), Yu-Long Fang(房玉龙), Shu-Jun Cai(蔡树军)

Chin. Phys. B, 2016, 25 (**10**): 107106. DOI: 10.1088/1674-1056/25/10/107106

Breakdown mechanisms in AlGaN/GaN high electron mobility transistors with different GaN channel thickness values

Ma Xiao-Hua (马晓华), Zhang Ya-Man (张亚嫚), Wang Xin-Hua (王鑫华), Yuan Ting-Ting (袁婷婷), Pang Lei (庞磊), Chen Wei-Wei (陈伟伟), Liu Xin-Yu (刘新宇)

Chin. Phys. B, 2015, 24 (**2**): 027101. DOI: 10.1088/1674-1056/24/2/027101

A novel Si-rich SiN bilayer passivation with thin-barrier AlGaN/GaN HEMTs for high performance millimeter-wave applications

Zhihong Chen(陈治宏)[1], Minhan Mi(宓珉瀚)[1,3,†], Jielong Liu(刘捷龙)[2], Pengfei Wang(王鹏飞)[1], Yuwei Zhou(周雨威)[2], Meng Zhang(张濛)[1], Xiaohua Ma(马晓华)[1], and Yue Hao(郝跃)[1]

[1] *Key Laboratory of Wide Band-Gap Semiconductor Materials and Devices, School of Microelectronics, Xidian University, Xi'an* 710071, *China*
[2] *School of Advanced Materials and Nanotechnology, Xidian University, Xi'an* 710071, *China*
[3] *Guangzhou Institute of Technology, Xidian University, Guangzhou* 510555, *China*

(Received 31 May 2022; revised manuscript received 11 July 2022; accepted manuscript online 18 July 2022)

We demonstrate a novel Si-rich SiN bilayer passivation technology for AlGaN/GaN high electron mobility transistors (HEMTs) with thin-barrier to minimize surface leakage current to enhance the breakdown voltage. The bilayer SiN with 20-nm Si-rich SiN and 100-nm Si_3N_4 was deposited by plasma-enhanced chemical vapor deposition (PECVD) after removing 20-nm SiO_2 pre-deposition layer. Compared to traditional Si_3N_4 passivation for thin-barrier AlGaN/GaN HEMTs, Si-rich SiN bilayer passivation can suppress the current collapse ratio from 18.54% to 8.40%. However, Si-rich bilayer passivation leads to a severer surface leakage current, so that it has a low breakdown voltage. The 20-nm SiO_2 pre-deposition layer can protect the surface of HEMTs in fabrication process and decrease Ga–O bonds, resulting in a lower surface leakage current. In contrast to passivating Si-rich SiN directly, devices with the novel Si-rich SiN bilayer passivation increase the breakdown voltage from 29 V to 85 V. Radio frequency (RF) small-signal characteristics show that HEMTs with the novel bilayer SiN passivation leads to f_T/f_{max} of 68 GHz/102 GHz. At 30 GHz and $V_{DS} = 20$ V, devices achieve a maximum P_{out} of 5.2 W/mm and a peak power-added efficiency (PAE) of 42.2%. These results indicate that HEMTs with the novel bilayer SiN passivation can have potential applications in the millimeter-wave range.

Keywords: AlGaN/GaN HEMTs, thin-barrier, Si-rich SiN passivation, current collapse, surface leakage current, millimeter-wave

PACS: 71.55.Eq, 73.20.–r, 73.50.–h **DOI:** 10.1088/1674-1056/ac81a6

1. Introduction

Due to the excellent features, such as high breakdown field (3.3 MV/cm), high electron saturation velocity (2.5×10^7 cm/s) and wide bandgap (3.4 eV), GaN-based high electron mobility transistors (HEMTs) have potential in radio frequency (RF) and millimeter-wave applications.[1–4] However, for millimeter-wave devices with thin-barrier, the polarization effect decreases and the concentration of two-dimensional electron gas (2DEG) on the GaN side of the AlGaN/GaN heterojunction interface is much lower than that of the conventional barrier structure, thus the current of the devices is poor and the saturation current is low.[5] In addition, thin-barrier HEMTs have a problem of severe surface leakage current after using the conventional Si_3N_4 passivation process, which can cause the breakdown voltage of the device decrease, as well as the current collapse effect.[6,7] Some reports have confirmed that current collapse is caused by traps on the device surface.[8,9] When the traps locate between gate and drain access region, it will exist a second virtual gate, which will deplete 2DEG.[10–12] With the decrease of barrier thickness, surface traps have more effect for 2DEG in the channel. Because of the increase in the electric fields in thin-barrier HEMTs, current collapse will become more serious.[13]

For ordinary GaN HEMTs, current collapse has been well suppressed in various methods.[14–16] It is no doubt that passivation is the most commonly used way to mitigate current collapse.[17–19] Bilayer SiN passivation technology has been studied in recent reports. This method can not only optimize DC performances like current collapse, but also improve small- and large-signal characteristics because it can be good used to decrease traps-related dispersive effects caused by electron trapping. In 2015, Huang *et al.* reported that HEMTs with bilayer SiN passivation with Si-rich SiN can decrease the current collapse ratio to 3.31% at quiescent bias points $(V_{GS,Q}, V_{DS,Q}) = (-6\text{ V}, 24\text{ V})$ and obtained an output power density of 5.4 W/mm at 3 GHz.[20–22] In addition, by contrast to traditional Si_3N_4 passivation film, Si-rich SiN film has relatively more Si–H bonds because of the increasing of SiH_4 flow.[23] However, as for thin-barrier HEMTs, Si-rich SiN bilayer passivation has only suppressed current collapse in our previous research. Devices have a low breakdown voltage because of severe surface leakage current, which restricts their power application at high voltage.[24] The leakage current may be created by surface traps, which comes from plasma etching during the fabrication process.[25]

In this work, a novel Si-rich SiN bilayer passivation was deposited by plasma-enhanced chemical vapor deposition (PECVD) for AlGaN/GaN HEMTs with thin-barrier. Com-

†Corresponding author. E-mail: miminhan@qq.com
© 2022 Chinese Physical Society and IOP Publishing Ltd

pared to Si_3N_4 passivation, Si-rich SiN/Si_3N_4 bilayer passivation can not only increase 2DEG density, but also suppress current collapse ratio from 18.54% to 8.40% at the quiescent bias point $(V_{GS,Q}, V_{DS,Q}) = (-8\ \text{V}, 30\ \text{V})$. Nevertheless, it had an extremely low breakdown voltage of 29 V and a large surface leakage current. Based on these results, we fabricated HEMTs with Si-rich SiN bilayer passivation after removing SiO_2 pre-deposition layer. This novel bilayer passivation technology can effectively decrease surface traps and surface leakage current, so that suppress current collapse and enhances the breakdown voltage. The fabricated devices can obtain an f_T/f_{max} of 68 GHz/102 GHz at $V_{DS} = 6$ V, and demonstrate an output power density (P_{out}) of 5.2 W/mm and a peak power-added efficiency (PAE) of 42.2% at 30 GHz and $V_{DS} = 20$ V. The off-state stress measurement results show that HEMTs have nearly no degradation in saturation current and peak transconductance at $V_{gstress} = -5$ V, $V_{dstress} = 40$ V and $t_{stress} = 1000$ s, denoting that devices have a long-term reliability. These results indicate that this novel passivation technology can have a good use in millimeter-wave range for thin-barrier AlGaN/GaN HEMTs.

2. Device structure and fabrication

Two types of device schematic cross-sections with Si-rich SiN bilayer passivation are exhibited in Fig. 1. Devices in Fig. 1(a) were passivated with 20-nm Si-rich SiN (Si-rich SiN, SiH_4:NH_3 flow=450:2 sccm) and 100-nm Si_3N_4 (Si_3N_4, SiH_4:NH_3 flow=100:2 sccm). Devices with the novel Si-rich SiN bilayer passivation in Fig. 1(b) were passivated with 20-nm Si-rich SiN and 100-nm Si_3N_4 after removing SiO_2 pre-deposition layer. The AlGaN/GaN heterostructure of all devices was epitaxially grown on SiC substrate by metal–organic chemical vapor deposition (MOCVD). And the epilayers were consisted of 1.6-μm GaN buffer, 400-nm i-GaN layer, 1-nm AlN spacer layer, and 12-nm AlGaN barrier layer.

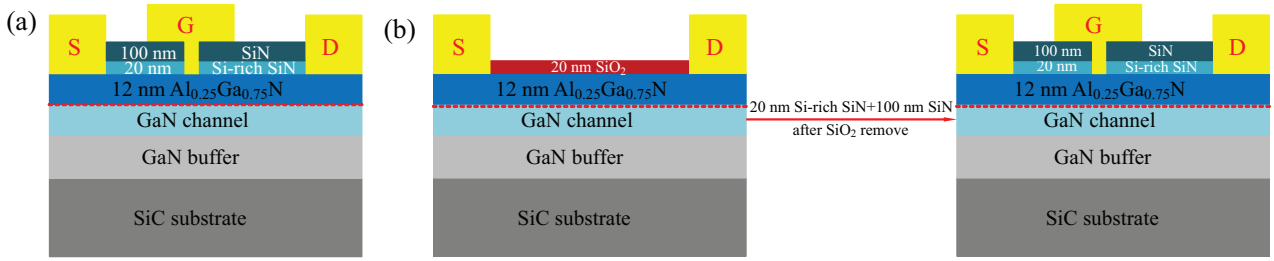


Fig. 1. Schematic diagram of AlGaN/GaN HEMTs with (a) Si-rich SiN bilayer passivation. (b) Si-rich SiN bilayer passivation after removing SiO_2 pre-deposition layer.

The only difference in device fabrication of HEMTs with the novel Si-rich SiN bilayer passivation is that it was deposited 20-nm SiO_2 layer at the first process. Ti/Al/Ni/Au ohmic contact was treated by the electron beam evaporation and rapid temperature annealing (RTA) at 830 °C for 60 s in N_2 ambient. The measured ohmic contact resistance (R_C) by transfer line measurement (TLM) was 0.39 Ω·mm. Device isolation was formed by nitrogen ion implantation. Then the SiO_2 pre-deposition layer was removed using hydrofluoric acid. Si-rich SiN/Si_3N_4 bilayer passivation was then deposited by PECVD. T-shaped gate was defined by electron-beam lithography (EBL), and etched by CF_4-based inductively coupled plasma (ICP) etching to remove SiN in the gate-foot. Finally, the Ni/Au gate electrode was deposited by electron beam evaporation. The gate length was 150 nm, the source-drain distance was 2 μm, and the gate width was 2×50 μm.

3. Results and discussion

3.1. Current collapse suppression

The DC transfer characteristics and TLM measurement results of AlGaN/GaN HEMTs with traditional Si_3N_4 and Si-rich SiN bilayer passivation are shown in Fig. 2. We can see from Fig. 2(a) that HEMTs with Si-rich SiN improved drain current (I_D) and peak transconductance (G_m) at $V_{DS} = 6$ V from 1057 mA/mm and 344 mS/mm to 1273 mA/mm and 408 mS/mm, respectively, compared to HEMTs with Si_3N_4 passivation. These results indicated that Si-rich SiN bilayer passivation could effectively increase 2DEG density, resulting in an improvement for current and transconductance. Meanwhile, as shown in TLM measurement results in Fig. 2(b), after passivating Si-rich SiN, R_{sheet} decreased from 334 Ω/□ to 277 Ω/□. The reduction of R_{sheet} was also benefited from the increase of 2DEG density.

On the other hand, Si-rich SiN bilayer passivation solved the current collapse for thin-barrier HEMTs. The *I*–*V* pulsed characteristics of HEMTs were measured by Keithley-4200 semiconductor parameter analyzer to investigate current collapse in Fig. 3, where the pulse width and pulse period were 500 ns and 1 ms, respectively. The quiescent bias points ($V_{GS,Q}$, $V_{DS,Q}$) were set (0 V, 0 V), (−8 V, 0 V), and (−8 V, 30 V). We can clearly find that HEMTs with Si_3N_4 passivation had a more serious current collapse ratio about 18.54% at the quiescent bias point (−8 V, 30 V). However, after passivating Si-rich SiN bilayer passivation, devices had an excellent current collapse performance. It reached only 0.35% and 8.40% current collapse ratio at the quiescent bias point (−8 V, 0 V) and (−8 V, 30 V), respectively. The mechanism of suppressing current collapse by Si-rich SiN passivation is that Si–H bonds are more due to the increased flow of the SiH_4. The excess

Si–H bonds tend to react with the oxygen elements on the device surface, thus reducing the surface state. The reduction of the surface state suppresses the RF scattering, resulting in the suppression of current collapse.[20,21,23]

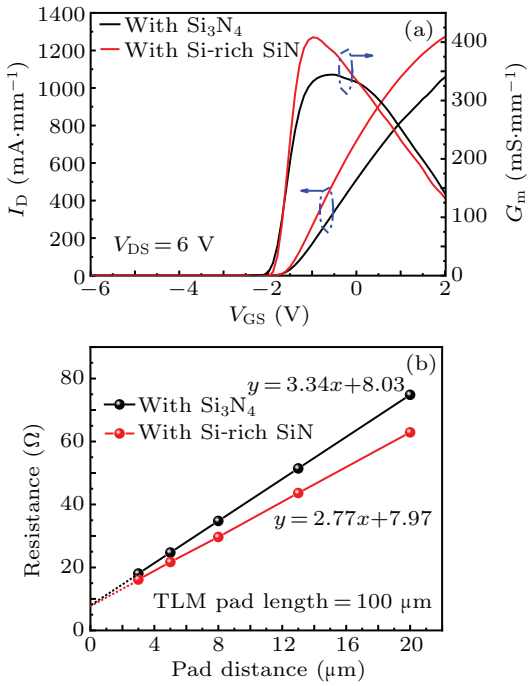


Fig. 2. (a) Transfer characteristics of HEMTs with Si_3N_4 and Si-rich SiN bilayer passivation. (b) TLM measurement results of HEMTs with Si_3N_4 and Si-rich SiN bilayer passivation.

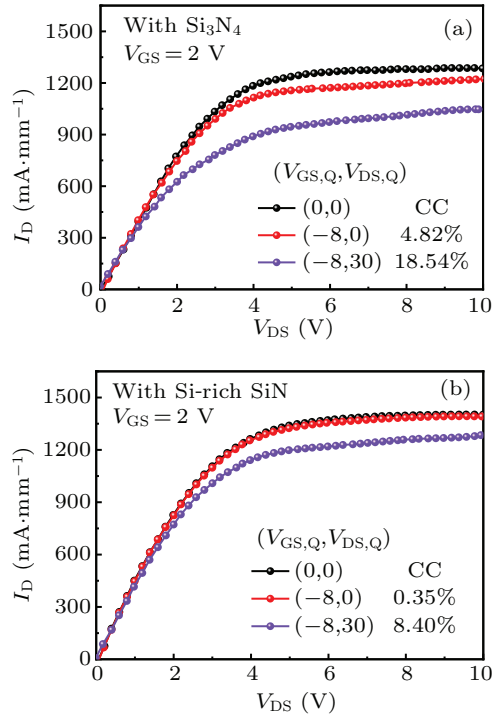


Fig. 3. The *I*–*V* pulsed characteristics of AlGaN/GaN HEMTs with (a) Si_3N_4 passivation. (b) Si-rich SiN bilayer passivation.

3.2. Surface leakage current suppression

To research the effect of SiO_2 pre-deposition on HEMTs with thin-barrier, we did the same fabrication process by Si_3N_4 passivation layer. The results of devices using four different types of passivation by Si_3N_4 and Si-rich SiN, which were with and without SiO_2 pre-deposition layer, were shown in Fig. 4. It was obvious that HEMTs with Si_3N_4 after SiO_2 remove still had a high current collapse. It only enhanced the breakdown voltage from 24 V to 81 V. And devices with Si-rich SiN after SiO_2 remove could have a low current collapse and a large breakdown voltage. We will explain the passivation in more detail below.

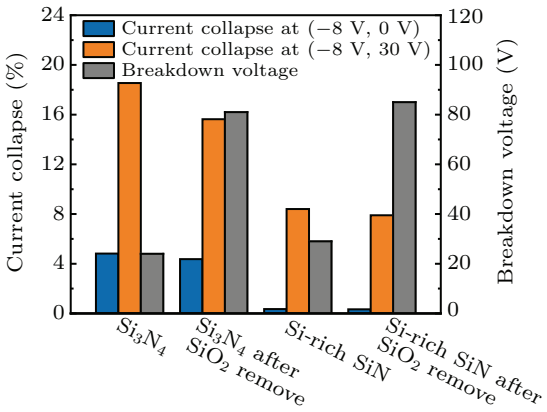


Fig. 4. Comparison of four types SiN passivation on current collapse and breakdown voltage.

Although Si-rich SiN bilayer passivation optimized current collapse for thin-barrier HEMTs, severe surface leakage current caused a very low breakdown voltage. The purpose of the novel bilayer passivation is to suppress surface leakage current. As shown in Fig. 5, after removing SiO_2 pre-deposition layer, HEMTs with Si-rich SiN bilayer passivation enhanced the breakdown voltage from 29 V to 85 V at $I_D = 1$ mA/mm. Dual gate was measured to analyze the mechanism of the enhancement of breakdown voltage. Figure 6 shows the dual gate structure of HEMTs with SiN passivation to distinguish surface leakage current and barrier leakage current. We fabricated another gate 2 by Schottky contact and a negative voltage sweeping was applied to gate 2. On the other hand, source and gate 1 were biased to 0 V, and monitored their current at the same time. It can be seen from the structure that gate 1 had the same potential with 2DEG because of $V_{\text{gate 1}} = 0$ V. The leakage current flowed from gate 1 must be surface current, and the barrier leakage current was monitored by the source terminal.[26,27] Figure 7 shows the characteristics of surface leakage current (I_S) with gate 2 voltage (V_{G2}) for HEMTs with two types of Si-rich SiN bilayer passivation. As shown in Fig. 7, it was obvious that different SiN passivation could efficiently effect surface leakage current. Compared to passivating Si-rich SiN/Si_3N_4 directly, HEMTs with Si-rich SiN/Si_3N_4 after removing SiO_2 pre-deposition layer suppressed surface leakage current from 2.5×10^{-3} mA/mm to 1.1×10^{-6} mA/mm at $V_{G2} = -50$ V. Almost three orders reduction of surface current illustrated that the novel SiN bilayer passivation suppressed the density of surface electronic states

and surface leakage current, thereby the breakdown voltage of the HEMTs had a great enhancement.

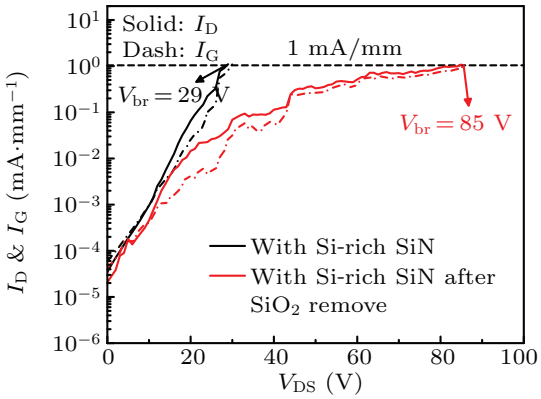


Fig. 5. Breakdown voltage (V_{br}) comparison of HEMTs with two types of Si-rich SiN bilayer passivation.

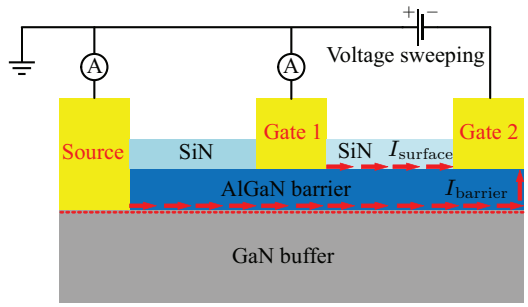


Fig. 6. Schematic diagram of dual gate structure.

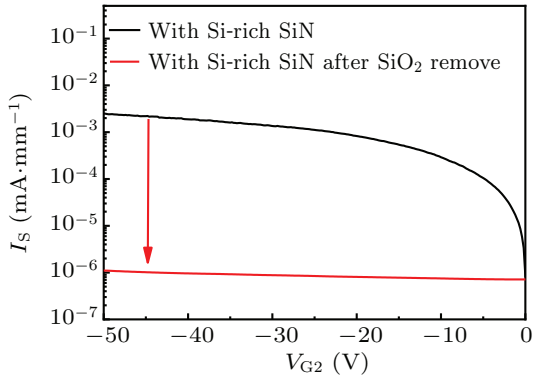


Fig. 7. Surface leakage current (I_S) of HEMTs HEMTs with two types of Si-rich SiN bilayer passivation.

The x-ray photoelectron spectroscopy (XPS) was measured to investigate the mechanism of the decrease of surface leakage current and the effect of device surface trap by two types of Si-rich SiN bilayer passivation. Figure 8 shows the Ga 3d core-level spectra of the AlGaN/SiN interface for two samples, respectively. Ga–O bonds and Ga–N bonds were separated from Ga 3d peaks. In contrast to Si-rich SiN sample, the intensity of Ga–O peak in devices with Si-rich SiN after removing SiO_2 pre-deposition layer had an obvious reduction. The concentration of Ga–O bond in Ga 3d peak can be seen as a marker to qualitatively analyze surface traps content. Thus the decline of Ga–O peak indicates that surface traps was removed by SiO_2 pre-deposition treatment and passivating Si-rich SiN.[28] Meanwhile, surface traps are also closely related to surface leakage current and breakdown voltage. When the surface traps filled with injected electrons, the depletion region along the channel will be extended, resulting in an electric field peak at the drain-side gate edge. So the surface leakage current and the breakdown voltage have an improvement.[29,30]

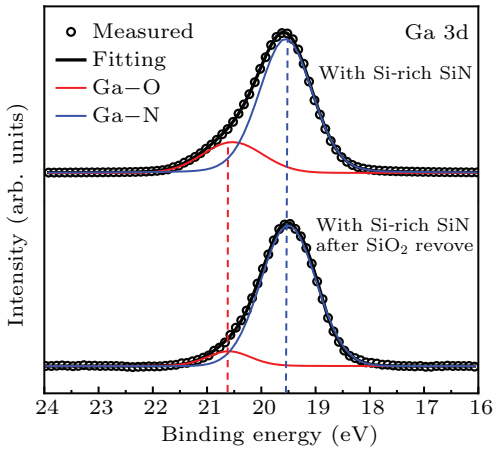


Fig. 8. The XPS spectra of Ga 3d for HEMTs with three types of bilayer SiN passivation.

3.3. Small- and large-signal characteristics

The RF small-signal characteristics of HEMTs with the novel bilayer SiN passivation were achieved by Agilent-8363B network analyzer within the frequency from 100 MHz to 40 GHz. The current gain extrinsic cut-off frequency (f_T) and the maximum oscillation frequency (f_{max}) were obtained by short open-load-through calibration standard at 40 GHz. Figure 9 shows the unilateral power gain (UPG), maximum stable gain (MSG), and current gain $|H_{21}|^2$ as a function of frequency for sample 3 at $V_{DS} = 6$ V and $V_{GS} = -1.8$ V. After extrapolating the short circuit current gain ($|H_{21}|^2$) and the unilateral power gain (UPG) curves through using -20 dB/decade slope, the f_T/f_{max} of sample 3 with Si-rich SiN after removing SiO_2 had a value of f_T/f_{max} of 68 GHz/102 GHz.

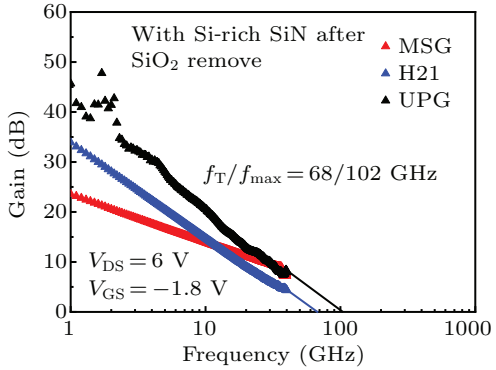


Fig. 9. The RF small-signal characteristics of AlGaN/GaN HEMTs with Si-rich SiN bilayer passivation after removing SiO_2 pre-deposition layer.

To verify the application of HEMTs with the novel bilayer SiN passivation in millimeter-wave range and their power characteristics, large-signal power measurement was treated at 30 GHz in continuous-wave (CW) mode. The source and load

impedances were tuned to obtain maximum power-added efficiency (PAE). The device was biased at class-AB. At V_{DS} = 20 V, as shown in Fig. 10, the PAE, the power gain (gain), and output power density (P_{out}) were a function of the input power (P_{in}), respectively. Sample 3 with the novel bilayer SiN passivation had a maximum P_{out} of 5.2 W/mm and a peak PAE of 42.2%. In millimeter-wave range, the power measurement results demonstrated that HEMTs with the novel bilayer SiN passivation can have excellent applications in Ka-band.

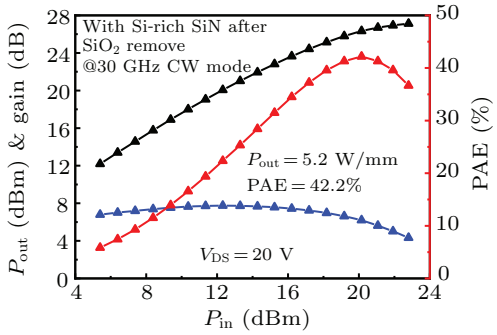


Fig. 10. Large-signal characteristics of the HEMTs with Si-rich SiN bilayer passivation after removing SiO_2 pre-deposition layer at 30-GHz CW mode.

4. Conclusions

In summary, AlGaN/GaN HEMTs with 20-nm Si-rich SiN and 100-nm Si_3N_4 passivation after removing SiO_2 pre-deposition layer extraordinarily optimize device performances. This novel bilayer SiN passivation technology solves surface leakage current for thin-barrier GaN-based HEMTs with conventional passivation. HEMTs with this novel passivation can not only suppress current collapse to 8.40% at the quiescent bias point (−8 V, 30 V), but also decrease surface leakage current to 1.1×10^{-6} mA/mm, so that enhance the breakdown voltage to 85 V. Furthermore, RF small-signal measurement shows that devices with this type of passivation obtain f_T/f_{max} of 68 GHz/102 GHz. At 30-GHz CW mode, V_{DS} = 20 V, HEMTs have a maximum P_{out} of 5.2 W/mm and a peak PAE of 42.2%. These results indicate that AlGaN/GaN HEMTs with the novel Si-rich SiN bilayer passivation technology can have better applications in high voltage and millimeter-wave range.

Acknowledgements

Project supported by the National Key Research and Development Program of China (Grant No. 2020YFB1804902), the National Natural Science Foundation of China (Grant Nos. 61904135, 62090014, and 11690042), the Fundamental Research Funds for the Central Universities, the Innovation Fund of Xidian University (Grant No. YJS2213), the China Postdoctoral Science Foundation (Grant Nos. 2018M640957 and BX20200262), the Key Research and Development Program of Guangzhou (Grant No. 202103020002), Wuhu and Xidian University Special Fund for Industry–University-Research Cooperation (Grant No. XWYCXY-012021014-HT), and the Fundamental Research Funds for the Central Universities, China (Grant No. XJS221110).

References

[1] Chung J W, Hoke W E, Chumbes E M and Palacios T 2010 *IEEE Electron Dev. Lett.* **31** 195
[2] Lee D S, Liu Z H and Palacios T 2014 *Jpn. J. Appl. Phys.* **53** 100212
[3] Cakmak H, Ozturk M, Ozbay E and Imer B 2021 *IEEE Trans. Electron Dev.* **68** 1006
[4] Zhang Y C, Huang S, Wei K, Zhang S, Wang X H, Zheng Y K, Liu G G, Chen X J, Li Y K and Liu X Y 2020 *IEEE Electron Dev. Lett.* **41** 701
[5] Khan M A, Chen Q, Sun C J, Yang J W, Blasingame M, Shur M S and Park H 1996 *Appl. Phys. Lett.* **68** 514
[6] Kohn E, Daumiller I, Schmid P, Nguyen N X and Nguyen C N 1999 *Electron. Lett.* **35** 1022
[7] Eastman L F 1999 *Physica Status Solidi A* **176** 175
[8] Huang T D, Bergsten J, Thorsell M and Rorsman N 2018 *IEEE Trans. Electron Dev.* **65** 908
[9] Huang T D, Axelsson O, Bergsten J, Thorsell M and Rorsman N 2020 *IEEE Trans. Electron Dev.* **67** 2297
[10] Vetury, Ramakrishna, Zhang and Naiqain Q 2001 *IEEE Trans. Electron Dev.* **48** 560
[11] Green B M, Chu K K, Chumbes E M, Smart J A, Shealy J R and Eastman L F 2000 *IEEE Electron Dev. Lett.* **21** 268
[12] Klein P B, Binari S C, Ikossi-Anastasiou K, Wickenden A E, Koleske D D, Henry R L and Katzer D S 2001 *Electron. Lett.* **37** 661
[13] Tilak V, Green B, Kaper V, Kim H, Prunty T, Smart J, Shealy J and Eastman L 2002 *IEEE Electron Dev. Lett.* **22** 504
[14] Wang X H, Huang S, Zheng Y K, Wei K, Chen X J, Liu G G, Yuan T T, Luo W J, Pang L, Jiang H J, Li J F, Zhao C, Zhang H X and Liu X Y 2015 *IEEE Electron Dev. Lett.* **36** 666
[15] Hasan M T, Asano T, Tokuda H and Kuzuhara M 2013 *IEEE Electron Dev. Lett.* **34** 1379
[16] Long R D, Hazeghi A, Gunji M, Nishi Y and McIntyre P C 2012 *Appl. Phys. Lett.* **101** 241606
[17] Liu Z H, Ng G I and Arulkumaran S 2009 *IEEE Electron Dev. Lett.* **30** 1122
[18] Gatabi I R, Johnson D W, Woo J H, Anderson J W, Coan M R, Piner E L and Harris H R 2013 *IEEE Trans. Electron Dev.* **60** 1082
[19] Tang Z K, Huang S, Jiang Q M, Liu S H, Liu C and Chen K J 2013 *IEEE Electron Dev. Lett.* **34** 366
[20] Liu J L, Mi M H, Zhu J J, Liu S Y, Wang P F, Zhou Y W, Zhu Q, Wu M, Lu H, Hou B, Wang H, Cai X L, Zhang Y, Duan X Y, Yang L, Ma X H and Hao Y 2021 *IEEE Trans. Electron Dev.* **69** 631
[21] Huang T D, Malmros A, Bergsten J, Gustafsson S, Axelsson O, Thorsell M and Rorsman N 2015 *IEEE Electron Dev. Lett.* **36** 537
[22] Kikkawa T, Iwai T and Ohki T 2008 *Fujitsu Science Technology* **44** 333
[23] Makiyama K, Ohki T, Okamoto N, Kanamura M, Masuda S, Nakasha Y, Joshin K, Imanishi K, Hara N, Ozaki S, Nakamura N and Kikkawa T 2011 *Physica Status Solidi (c)* **8** 2442
[24] Minko A, Hoel V, Morvan E, Grimbert B, Soltani A, Delos E, Ducatteau D, Gaquiere C, Theron D, De Jaeger J C, Lahreche H, Wedzikowski L, Langer R, Bove P and Bove P 2004 *IEEE Electron Dev. Lett.* **25** 453
[25] Lin Y S, Lain Y W and Hsu S S H 2010 *IEEE Electron Dev. Lett.* **31** 102
[26] Kotani J, Tajima M, Kasai S and Hashizume T 2007 *Appl. Phys. Lett.* **91** 093501
[27] Tan W S, Uren M J, Houston P A, Green R T, Balmer R S and Martin T 2006 *IEEE Electron Dev. Lett.* **27** 1
[28] Lin S X, Wang M J, Xie B, Wen C P, Yu M, Wang J Y, Hao Y L, Wu W G, Huang S, Chen K J and Bo S 2015 *IEEE Electron Dev. Lett.* **36** 757
[29] Zhao Z Q, Liao D W and Du J F 2012 *IEEE 11th InternationalConference on Solid-State and Integrated Circuit Technology*, October 29–November 1, 2012, Xi'an, China, p. 1
[30] Zhang N Q, Moran B, Denbaars S P, Mishra U K and Ma T P 2001 *International Electron Devices Meeting. Technical Digest* (Cat. No. 01CH37224), December 2–5, 2001, Washington, DC, USA, p. 5